

Design, Evaluation and Analysis of a Novel H-Shaped Capacitive RF MEMS Switch

Shoukathvali Khan

Koneru Lakshmaiah Education Foundation

K. Srinivasa Rao (✉ srinivasakarumuri@gmail.com)

Koneru Lakshmaiah University

Koushik Guha

National Institute of Technology Silchar

Research Article

Keywords: RF MEMS, Pull-In Voltage, Isolation, Insertion loss, Return loss, CPW, FOM

Posted Date: November 30th, 2021

DOI: <https://doi.org/10.21203/rs.3.rs-695902/v1>

License: © ⓘ This work is licensed under a Creative Commons Attribution 4.0 International License.

[Read Full License](#)

Design, Evaluation and Analysis of a Novel H-shaped Capacitive RF MEMS Switch

Shoukathvali Khan¹, K.Srinivasa Rao^{1*}, Koushik Guha²

¹MEMS Research Center, Department of Electronics and Communication Engineering, Koneru Lakshmaiah Education Foundation (Deemed to be University), Green Fields, Vaddeswaram-522502, Guntur, Andhra Pradesh, India

²National MEMS Design Center, Department of Electronics and Communication Engineering, National Institute of Technology Silchar, Assam, India

*The corresponding author e-mail address; srinivasakarumuri@gmail.com

Abstract: In this paper, absolute evaluation of Radio Frequency Micro Electromechanical System (RF MEMS) to improve parameters like high actuation voltage and low switching time, by introducing a new fixed - fixed RF MEMS capacitive switch. The proposed switch designed step-by-step evaluation of the plane beam, a novel structure of beam, and deposit the perforations and meanders to reduce the pull-in voltage. All the RF MEMS switch design parameters are studied using the COMSOL Multiphysics FEM (Finite Element Model) tool. The proposed RF MEMS switch expresses low pull-in voltage of 4.75V and good return, insertion, and isolation losses in both upstate and downstate conditions are >10dB, below 0.1dB and 60dB, respectively. The dielectric layer as silicon nitride (Si_3N_4), beam as a gold material. The RLC values are extracted by using lumped model design. The RF MEMS shunt switch (capacitance, inductance, and resistance) of the MEMS bridge are accurately evaluated from the S-parameter analysis. The computational and simulated results are in good agreement with each other, which indicates the validity of the proposed switch for K (18-26) GHz band applications.

Key words: RF MEMS, Pull-In Voltage, Isolation, Insertion loss, Return loss, CPW, FOM,

1 Introduction

The importance of the Radio Frequency Micro Electromechanical System (RF MEMS) improved over the last two decades. MEMS components exhibit good performance at RF frequency. The miniaturization of the devices possible by using MEMS technology (Rebeiz G. M. 2004). The solid-state switches like pin diodes and FET switches are replaced with the RF MEMS switches because of its advantages like high isolation, low weight, small in size, low power losses, and low cost. The traditional switches show very poor performance at a high frequency such as poor isolation, more power dissipation, high insertion, return losses, and the size of the structure is very large (Sharma et al. 2013). Each MEMS system consists of both electrical and mechanical configurations. Switch matrices with low power consumption and high isolation are an important element in satellite communication systems, so RF MEMS switches are the best choice for satellite communication matrices. There are two categories of RF MEMS switches: ohmic and shunt. Initially, an ohmic switch is in the off state, and no signal is passed through the transmission line; when the switch is activated, the signal is passed in downstate (on the state), the transmission signal is an electrical signal in an ohmic switch. The transmission

signal is an RF signal in shunt switch, and the signal cannot cross through the CPW line when the switch is upstate, by applying electrical voltage switch is closed, then the signal passed through the switch, to the ground. The ohmic switches have some advantages over the shunt switches as low pull-in voltage and high switching speed, the main drawback of these is ohmic switches has some restriction and reliability issues. Shunt switches are offered more pull-in voltage less switching speed (Rebeiz G M & Muldavin J. B. 2001). Electrostatic, electromechanical, piezoelectric, electromagnetic, and electrothermal are the different actuation mechanisms present to actuate the RF MEMS switches (Daneshmand M et al. 2009).

The electrostatic mechanism is the best way to actuate due to low power consumption, small size, and better switching time; the main failure is the more actuation voltage required to actuate the RF MEMS switch. RF MEMS switches have various applications in different fields such as reconfigurable antennas, filter mixture, switching networks, phased array radars, and RF phase shifter (Sharma Kuldeep et al. 2020). A thin dielectric layer is placed between the top and bottom electrodes, which provides isolation. Generally, Si_3N_4 ($\epsilon_r=7.5$) is used as a dielectric. Depending on the application different other dielectric materials present with high dielectric constants such as HfO_2 ($\epsilon_r=25$), AlN ($\epsilon_r=9.8$),

PZT($\epsilon_r=190$) and STO($\epsilon_r=190$). RF MEMS shunt switches act as two states of the digital capacitor: producing low capacitance in the upstate position (fF) and high capacitance in the downstate position(pF). The ratio of upstate capacitance and downstate capacitance (C_d/C_{up}) is known as the figure of merit (FOM) (**Koutsourelis M et al.2014**).

RF MEMS shunt switches are suitable for a high-frequency range that is $> 10\text{GHz}$. When the switch is actuated, these switches are shown a less parasitic effect. The changing capacitance varies the shunt switches' impedance; the switch focuses ON state a large gap between the two electroplates, leading to small capacitance results high impedance between the signal and ground. The switch is in OFF position a small dielectric layer presents between the two electroplates, which leads to large off-state capacitance, thus resulting in high impedance between the signal and ground (**Chakraborty et al.2017**). In the last two decades, different structures of RF MEMS switches come about designed, fabricated, and characterized. For example, electrostatic mechanism design of an RF MEMS shunt switch to achieve a high-power handling capacity of 0.8W , low actuation voltage of 6v , and -0.17 dB in insertion losses, by using push-pull and serpentine beam configuration but the isolation is not that high (-15.5 dB @ 40 GHz . $8\text{-}10\text{v}$ low actuation voltage achieved and maintaining the high-power capability by using symmetric toggle mechanism (**Peroulis et al.2004**).

The common method to use improve the capacitance ratio is to increase the air gap between the signal line and beam, which results in the switch excellent RF performances and high actuation voltage is required. The first method to decrease actuation voltage is, selecting the proper shape of the membrane or structure, but it is very difficult to fabricate the different membrane shapes. The second-best method to reduce the actuation voltage is, selecting the insulator having high dielectric constant such as Al_2O_3 , TlO_2 , SrTiO_3 instead of ordinary insulators like SiO_2 and AlN . High dielectric materials produce drastic improvement in the capacitance ratio including high dielectric charge, which affects the reliability. The RF MEMS switch isolation characteristics are low due to the more intermediation arise due to the other channel signal leakage, which results in reduced RF performance (**Majumder S et al. 2003**). In recent years different RF MEMS switches are designed and fabricated. An RF MEMS switch proposed with an air gap of $2\mu\text{m}$ on silicon substrate shows the isolation of about 25dB at 9GHz and returns loss less than 10dB (**Topalli K et al.2009**). MEMS shunt switch designed with an air gap of $2\mu\text{m}$ with the thickness of the gold membrane is $0.5\mu\text{m}$, that shows the insertion and isolation losses are 47.63dB , 0.5dB , and the actuation voltage is 4.8v . The RF MEMS switch shows the return losses of 0.034dB and isolation of 41dB at a frequency of 21GHz , and the actuation voltage is 9.7V (**Sravani K G et al. 2020**).

The main challenges in RF MEMS shunt capacitive switches are high actuation voltage, low mechanical stability, low power transmission, high stress on the beam, and low switching voltage. This can be lower the lifetime of the switch. The low actuation voltage will be obtained by taking low spring constant meanders deals with the device reliability and switching speed. The push-pull mechanism was also investigated on RF MEMS switches, but this method required high actuation voltage (**Ansari, Hamid Reza et al.2019**). Three different structures are proposed to achieve low actuation voltage varied between the 6 to 14V and shows good RF losses, including isolation from 70dB to 76dB and showing insertion losses from 0.005dB to 0.06dB at 10GHz (**Ansari, Hamid Reza et al.2019**). The actuation voltage of the RF MEMS switches can be further reduced with different shapes of the beam and with different meander techniques. The metal-to-metal contact RF MEMS switches show the upstate (off state) capacitance in the range of $2\text{-}10\text{ pF}$, which produces large isolation in the range of $20\text{-}40\text{dB}$. The shunt contact RF MEMS switches shows the down (off state) capacitance in the range of $1.4\text{-}3.5\text{pF}$, producing high isolation at resonant frequencies (**Sharma A K et al. 2013**). The RF MEMS switch electrical characterization can be done using the CLR model and the CLR model RF performance are determined by S-parameters. A similar approach is applied to find the electromagnetic model parameter for the proposed RF MEMS switch. The electrical parameters of the proposed switch are measured from S- parameters.

This paper reports evaluating a new structure RF MEMS capacitive switch with low actuation voltage and shows good RF performances. In this evaluation process, all the design parameters of a switch is observed for the normal plane beam, new shaped beam with different perforations and meandering technique. An electromechanical analysis is verified using the COMSOL FEM tool and RF performance analysis verified by HFSS. The rest of the paper will be as follows: The evaluation of the MEMS switch is explained in section 2, the results and discussion are shown in section 3, followed by the conclusion in section 4.

2. The Evaluation Process of RF MEMS Switch

2.1 Working mechanism and description of RF MEMS

The Silicon as the substrate with $\epsilon_r= 11.9$, the main advantage of silicon robustness has high applicability at high temperatures. A CPW line is placed over the substrate with the height of $1\mu\text{m}$, the gap between the signal line and ground is $37.5\mu\text{m}$, and the width of the signal line is $100\mu\text{m}$ with an impedance of 50Ω . To avoid the striction problem, a thin Si_3N_4 dielectric layer which shows a high dielectric constant, is placed over a central conductor with a height of $0.3\mu\text{m}$. Two actuation plates are placed in the gap between the signal line and the ground, with a height of $1\mu\text{m}$. The

membrane is suspended over a signal line with a gap of $2\mu\text{m}$ between the signal line and beams with anchors help. Initially, there is no biasing voltage. A small amount of capacitance is present between the signal line and beam in orders of femtofarads, which will not affect the RF signal flow. The maximum amount of signal will flow from the input port to the output port. ON state position of switch is shown in Fig.1, electrostatic force generated while applying the actuation voltage. This force pulls the beams towards the actuation pads and collapses on the signal line known as OFF-state of the switch position; a large amount of capacitance will be induced between the signal line and beam (Narayana et al. 2017). No RF signal would be transmitted from the input port to the output port in the off-state position. The off-state position of the RF signal is shown in Fig.2.

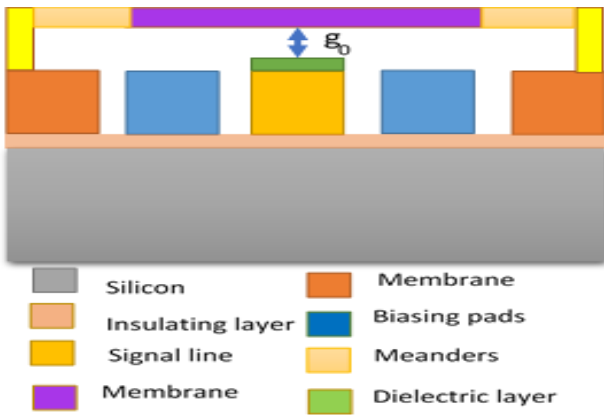


Fig.1 On state position of RF MEMS switch

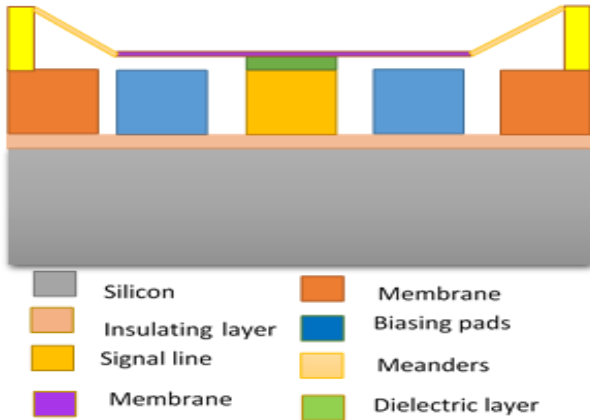


Fig.2 Off state position of RF MEMS switch

2.2 Normal Plane Beam RF MEMS Switch

The pull-in voltage of the switch depends on the dimensions and materials of the membrane, the design of a normal plane beam is shown below Fig.3. The length and width of the beam is $300\mu\text{m}$ and $100\mu\text{m}$, respectively. The plane beam is placed at the height of a $2\mu\text{m}$ from the signal line. There is no bias voltage between the electrodes and beam, a large gap is present between the beam, and a signal line that results in a low capacitance induced between the signal line

and beam. This low capacitance in orders of femtofarad, results in high impedance. RF signal passes from input to output when the switch is in the ON state. When applied actuation voltage is greater than the pull-in voltage, the beam collapses on the signal line, with a thin dielectric layer present between the signal line and beam. High capacitance is present in terms of picofarad, which results in low impedance; no input signal appears at the output terminal in off-state condition

Table 1 The physical dimensions of the Normal plane RF MEMS shunt switch

Component	material	length	Width	height
substrate	Si	400	300	55.5
Beam	Au/Al	300	100	0.5
CPW(G/W/G)	Au	35	100	1
Dielectric	Si_3N_4	100	110	0.3-0.5

The normal plane beam is considered to design an RF MEMS shunt type switch in the proposed design. The RF MEMS shunt switch pull-in voltage depends on different parameters such as the beam spring constant, the gap between the beam and the signal line, and the overlapping area. Residual stress is the other important parameter of the beam, affecting the spring constant, resulting in a change in the pull-in voltage. The physical dimensions of the plane beam RF MEMS shunt switch are shown in Table1.



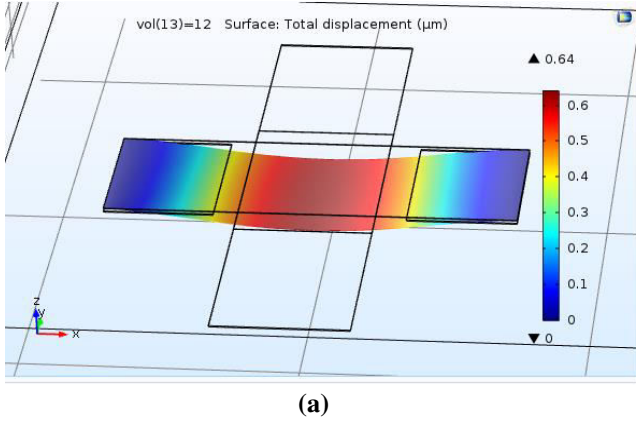
Fig.3 The schematic view of Plane beam structure

The minimum voltage required to pull down the beam to 1/3 of the air gap, the beam displacement occurred by the electrostatic force that applied the biasing voltage to the lower electrodes. The pull-in voltage of the proposed switch is calculated from Eq. (1).

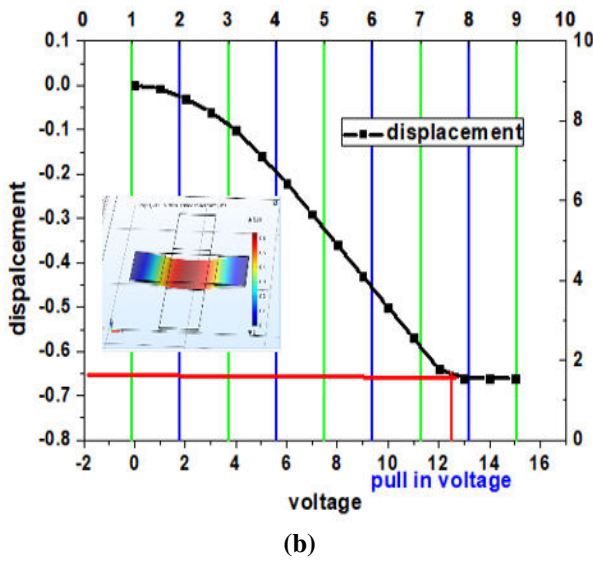
$$v_p = \sqrt{\frac{8Kg_0^3}{27\epsilon_0 A}} \quad (1)$$

The pull-in voltage of the switch depends on different parameters such as spring constant, air gap between the beam and signal line, and actuation area. The proposed switch beam and electrodes are designed using the FEM tool. The ends of the beam are fixed, and the membrane is the linear elastic boundary conditions, actuation voltage is applied to the electrodes, and the beam is grounded. The pull-in voltage of the proposed plane beam switch and the

displacement versus applied voltage of plane beam is shown in Fig.4.



(a)



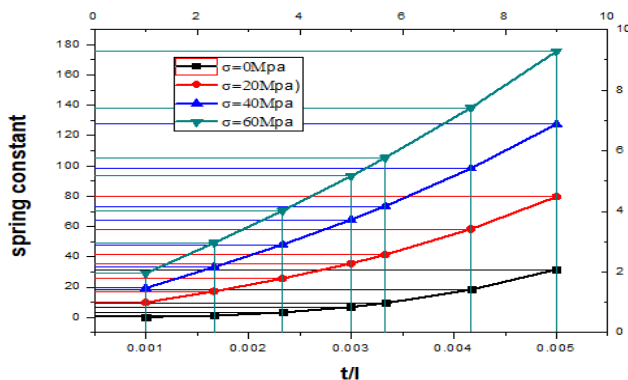
(b)

Fig.4a Pull-in voltage of plane beam, **b** Displacement of the plane beam with applied voltage

The spring constant of the beam offers the sum of the beam stiffness, and biaxial residual stresses from Eq.(2).

$$k_a = k'_a + k''_a = 32E \left(\frac{t}{l} \right)^3 + 8\sigma(1-\nu)w \left(\frac{t}{l} \right) \quad (2)$$

Where E is the young's module of beam material, w is the beam width, t is the beam thickness, l is the length of the beam, σ is the residual stress, ν is the poison ratio. Residual stress is one of the important parameters while calculating the spring constant.



The spring constant of the gold beam is calculated for various thickness to length ratios along with residual stress in the beam as shown below in Fig.5. The spring constant of the proposed switch is dominated by the residual stress component (K'') for $\sigma > 10 - 20MPa$.

Fig.5 Spring constant of the gold beam, versus residual stress in the beam

The critical stress of the beam depends on the young's module. Different materials are having different young's module values, which will impact the total spring constant value. The critical stress of the beam is calculated by using the Eq (3).

$$\sigma = \frac{\pi^2 Et^2}{3l^2(1-\nu)} \quad (3)$$

The pull-in voltage of plan beam depending on spring constant, air gap, and beam materials. Spring constant of different beam materials for various residual stress values are shown in Fig.5.

2.3 Shaped Beam RF Mems Switch

The plane beam is converted into H-shaped by etching 100 μ m length and 10 μ m width on beam shown in Fig.6. H-shaped beam exhibits low spring constant, high pull-in voltage, and less overlapping area that effects on capacitance. The capacitance ratio of the switch is defined as the ratio of downstate capacitance to upstate capacitance. The switch's RF performance depends on the capacitance ratio; a high capacitance ratio of the RF mems switch shows good RF performance. A high capacitance ratio will be achieved by getting the maximum capacitance in the downstate and minimum capacitance in the upstate position (Ansari, Hamid Reza et ai.2019).

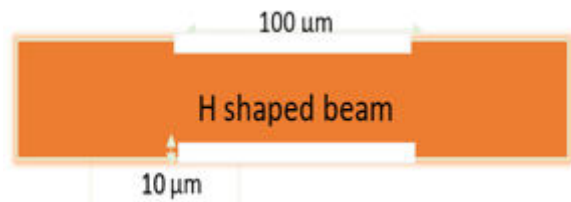
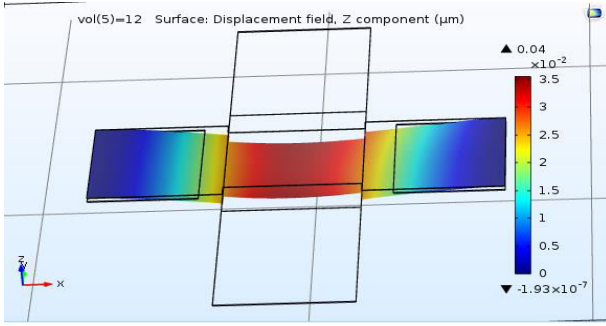
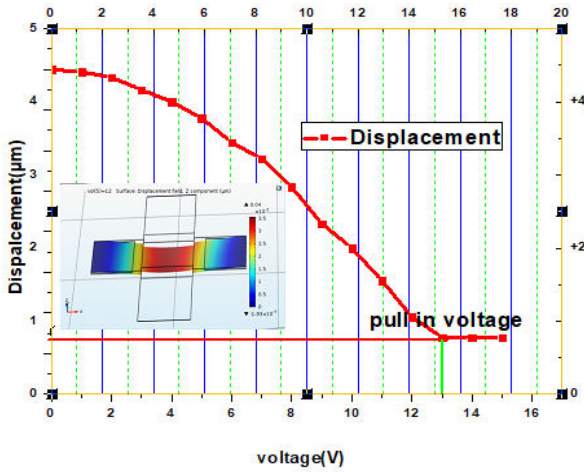


Fig.6 H Shaped RF MEMS switch

The upstate and downstate capacitance of the switch is measured by using Eq. (15) and (16). The proposed H-shaped switch has a low overlapping area that results in low upstate capacitance and decreases the capacitance ratio. The H-shaped switch shows good RF performance compared to the plane beam, as good isolation and low insertion losses.



(a)



(b)

Fig.7aSimulation of H- shaped beam, **b**Pull-in voltage calculation of H-shaped beam

2.4 H- Shaped Beam with Perforations

Many MEMS switches introduced had the holes on the beam with different dimensions (3-8 μ m) to reduce the squeeze film damping and increasing switching speed. The holes on the beam can occupy 60% of the area from the total area of beam. Performance of the beam is characterized when perforations are kept, by ligament efficiency $\mu=1/\text{pitch}$, where the pitch is the distance between the two consequent holes. Holes on the beams reduce the residual stress in the beam and reduces the young's module of the MEMS switch. Reduced residual stress is calculated by the Eq. (4).

$$\sigma = (1 - \mu) \sigma_0 \quad (4)$$

σ_0 is the residual stress without holes, μ is the ligament efficiency, 25% of young's module will be reduced for $\mu=0.16$, there is no effect on the upstate capacitance when the dimensions of the holes are less than (3-4 g_0), fringing fields that fill the area of the hole. On the other hand, downstate capacitance is affected by the holes that result, reduced in the capacitance ratio. High electric conductivity materials are exhibiting good isolation. The resonance frequency of the switch will be enhanced by taking low mass density materials. The resonance frequency of the beam is calculated by using Eq.(5).

$$\omega_0 = \sqrt{\frac{K}{m_{effect}}} \quad (5)$$

Where ω_0 is the resonance frequency, k is the spring stiffens coefficient, m_{effect} is the effective mass of the beam. If the switch's resonance frequency is increasing, then the switching time decrease accordingly, which results in improving the switching speed. The switching speed of the switch is calculated from Eq.(6).

$$t_s = \frac{3.67 v_p}{v_s 2 \Pi f_0} \quad (6)$$

Where t_s is the switching time, v_s is the actuation voltage ($v_s=1.4v_p$). Placing the holes on the beam, the effective mass of the beam is reduced then the resonance frequency is increasing, resulting in reduced switching time. Actuation voltage is applied between the beam and electrodes, an electrostatic force is generated that pulls the beam towards the lower electrodes. The air below the holes is out, which will make the pull-up and pull-down process of the switch very simple and easy. The main failure in increasing holes on the beam is, reduced the cross-sectional area that results in low isolation and reduced air damping effect. The damping coefficient of the beam can be calculated from Eq. (7).

$$b = \frac{3 \mu A_m^2}{2 \Pi g_0^3} \quad (7)$$

Where μ is the viscosity of the air ($1.88 \times 10^{-5} Pa$), A_m is the membrane area, g_0 is the airgap. Different kinds of perforations are kept on the beam such as square, circular, and rectangular as shown in Fig.8. The rectangular-shaped perforations achieved low pull-in voltage and spring constant (Saxena et al.2015).

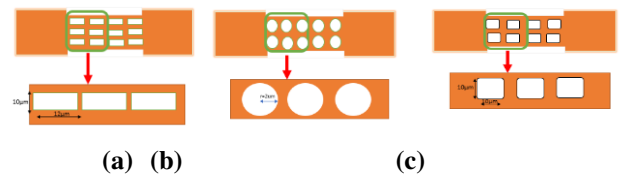
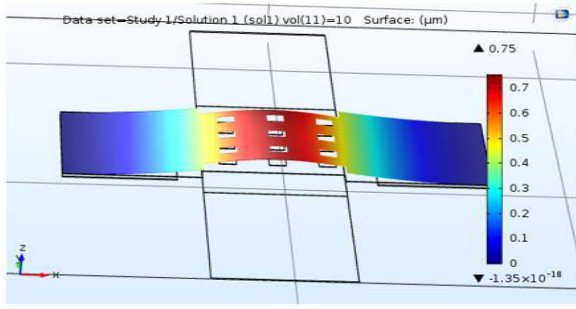
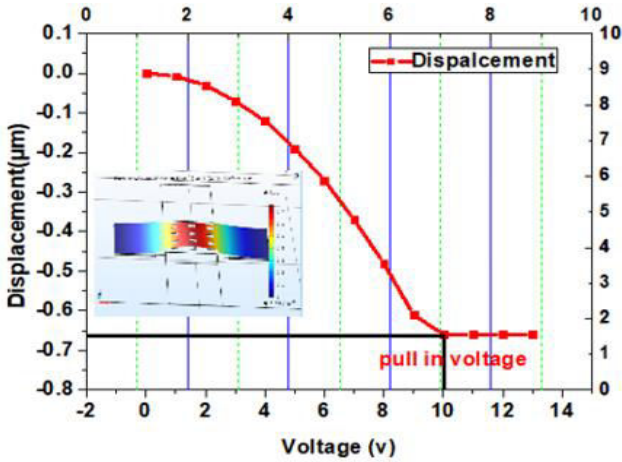


Fig.8Fixed-Fixed-beam with different perforations **a**square hole, **b**rectangular holes, **c**Circular holes

The pull-in voltage of the rectangularly perforated RF MEMS switch and the switch displacement verses applied voltage is shown in Fig.9. Pull-in voltage of rectangular perforations and the different types of the proposed perforations are shown in Fig.10. Comparing all pull-in voltage of the different beam's structures, H shaped beam along with rectangular perforations exhibited the lowest pull-in voltage.

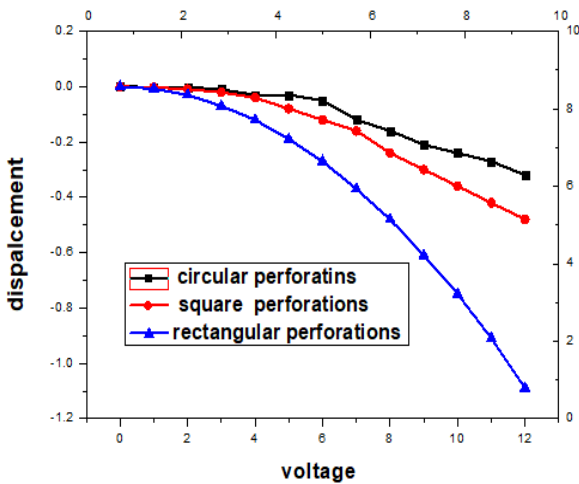


(a)



(b)

Fig.9a Pull- in voltage of H- shaped beam with rectangular perforations, **b** Displacement verses applied voltage of H- shaped beam with rectangular perforations



(a)

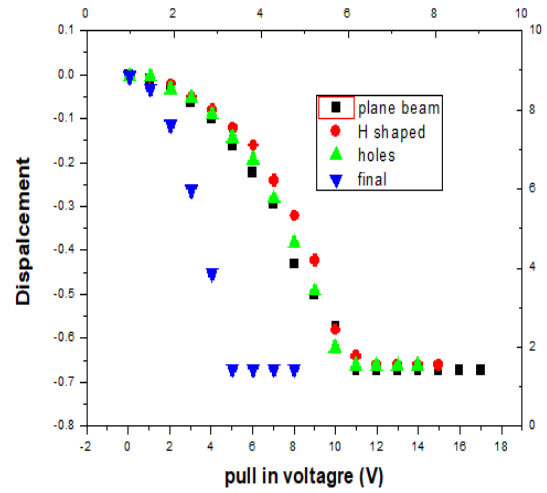


Fig.10a Voltage verse displacement of different perforations, **b** Pull- in voltage of different proposed switches

2.5 H-Shaped Beam with Meanders

The proposed design RF MEMS shunt switch with uniform meanders is presented in Fig.11. This proposed design has different layers; silicon (Si) is the lower layer that provides the platform to construct other components. A thin oxide layer is placed over a substrate layer, which protects the silicon substrate from the leakage currents and improves the switch RF performance. The proposed RF MEMS switch consists of a coplanar waveguide (CPW) over an oxide layer and which transmit the signal line. A DC actuation voltage is required to perform the ON/OFF operation of the switch. The coplanar waveguide has a signal line width of $100\mu\text{m}$, and the gap between the signal line and ground is $37.5\mu\text{m}$; some parts of the ground lines are etched to improve the impedance of the switch and revoke the stray capacitance. The switch performance depends on the membrane, main target of the membrane design is to have a low pull-in voltage, and different meandering techniques to achieve low spring constant value. Four anchors are placed over the ground to hold the membrane, and the membrane is placed over the signal line. Silicon nitride (Si_3N_4) as dielectric layer is placed over a signal line that forms the signal line and beam capacitance. Uniform meanders are used to suspend the beam over a signal line with a gap of $3\mu\text{m}$ between the beam and dielectric layer. Two metal actuated plates are placed on both sides of the signal line and below the membrane. These actuation pads are used to actuate the membrane during switching operations. The proposed switch dimensions and materials are shown in Table2. which operates on the K band frequency range.

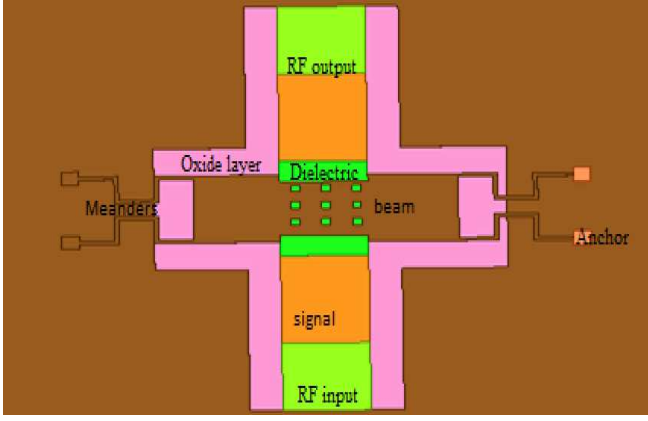


Fig.11 Schematic of the final proposed switch

The normal plane beam produces more pull-in voltage because of the centre beam's high stiffness (Peroulis, Dimitrios et al.2004) the meandering technique reduces the pull-in voltage; the proposed RF MEMS shunt switch membrane is suspended over CPW with the help of meanders. One end of the meanders is connected to the fixed anchor, and the other end is connected to the beam; each beam is having five individual beams $k_1, k_2, k_3, k_4,$ and k_5 as shown in Fig.12. The membrane is pulled down by electrostatic force, and meanders resist the membrane moment by their spring stiffens. The electrostatic force is present, the entire structure of RF MEMS switches along with meanders (Sravani.K.G et al.2020). The spring constant of the meanders depend on the size, shape, and young's modulus of the material.

Table 2 Device specification of final proposed RF MEMS switch

Sl.no	Component)	Length* Width* Depth (um)	Material
1	Substrate	775*640 *50	Silicon
2	Insulating layer	775*640 *0.5	SiO ₂
3	CPW (G/S/G)	37.5/100/ 2	Gold
4	Dielectric layer	100*140 *0.3	Si ₃ N ₄
5	Membrane	300*80* 0.5	Gold
6	Electrodes		Gold
7	Meanders	40*5*0.5	Gold
9	The gap between the signal to ground	0.2	



Fig.12 Square meanders

The square-type meanders produce a low spring constant along with low pull-in voltage (Chakraborty et al. 2014). The spring constant of the individual beam is calculated by Eq. (8).

$$K_b = \frac{Ewt^3}{l^3} \quad (8)$$

K_b is the constant of each part of spring, E is the young's, module value of meander, t,l,w are the thickness, length, and width of the meander, respectively.

$$\frac{1}{K_x} = \frac{1}{k_1} + \frac{1}{k_2} + \frac{1}{k_3} + \frac{1}{k_4} + \frac{1}{k_5} \quad (9)$$

$$\frac{1}{K_x} = \frac{5}{K_b} \quad (10)$$

$$K_{eff} = 4K_x \quad (11)$$

The proposed switch having 4 meanders, the total spring stiffens of the switch is calculated using Eq.(9). The individual beam has a spring stiffness of 0.17 N/m², and the whole switch has a spring stiffness of 0.7 N/m². The pull-in voltage of the proposed switch with square-type meanders and rectangular perforations showing low pull-in voltage is shown in Fig.15.

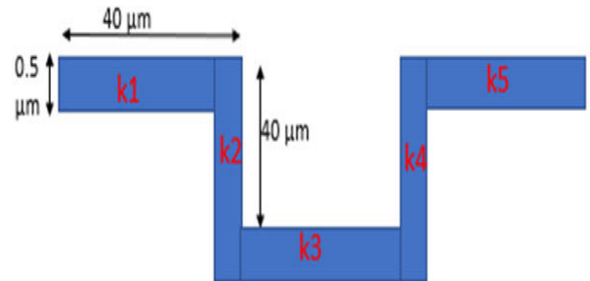


Fig.13 Single meander section in the proposed switch

2.6. Extraction of R, L, C Components

The resonant frequency of the RF MEMS shunt switch is varied by choosing a proper high impedance dimension. CLR mode of the proposed RF MEMS shunt switch is shown in Fig.14. bridge resistance, capacitance, and

inductance are the switch's three parameters. RF signal is passed by the switch through the signal line, when the switch is in ON state, and blocks the RF signal in OFF state (Sharma, A. K et al.2015). The impedance of the RF MEMS bridge is calculated from Eq.(12).

$$Z = \begin{cases} \frac{1}{\omega c} & f \leq f_0 \\ R & f=f_0 \\ j\omega L & f \geq f_0 \end{cases} \quad (12)$$

Eq. (12) comes from the CLR model and the MEMS bridge acts as a capacitor below the resonance frequency, as a resistor at resonant frequency and inductor above the resonant frequency. The MEMS bridge impedance mainly depends on the beam overlapping area to the gap between the signal line to ground and the MEMS bridge overlapping area. RF MEMS switch is characterized by using S-parameters analysis in both ON and OFF state of MEMS bridge. The RF MEMS shunt switch parameters are S_{11} , S_{21} are the return losses and insertion losses in upstate position and S_{21} , S_{11} isolate and return losses in downstate position. Resistance, inductance and capacitance play an important role while calculating the RF performance, such as insertion losses, return losses and isolation losses in both upstate and downstate positions.

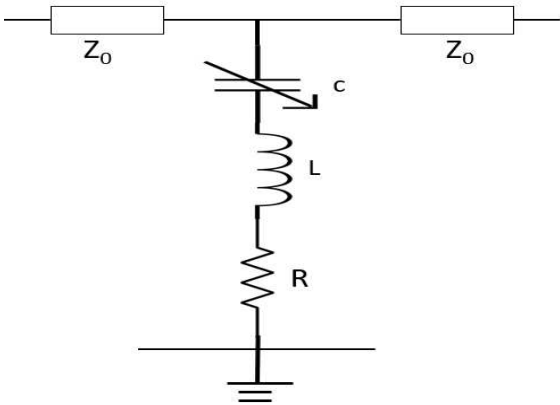


Fig.14 Lumped electrical model of proposed RF MEMS switch

Table 3 Comparison of analytical and simulated values RF MEMS switch

Switch Type	C_{up} calculated	C_{Down} calculated	C_{Down}/C_{up} calculated	Extracted Circuit Model (CLR) Parameter				C_{Down}/C_{up} Simulated
				C_{up}	C_{Down}	R_b	L_b	
Proposed RF MEMS shunt switch	35.2fF	2.6pF	73	37.2fF	2.8pf	2.41 Ω	21.9 pH	75

2.7 Parameter Extraction

This section represents the extraction of the proposed RFMEMS shunt switch. Simulated and calculated upstate and downstate capacitance and RLC parameters are shown in Table3. The upstate capacitance affects the return losses in on-state conditions, and electromagnetic analysis is done using the HFSS electromagnetic simulator tool from 0-50 GHz frequency range. The on-state capacitance value is extracted from simulated return losses at a frequency of 5GHZ, which is below the resonant frequency of 20GHZ. The MEMS bridge act as the capacitor below the resonant frequency; at 5GHZ, the RF MEMS switch exhibits the return losses of 25dB. This value of return losses provides the upstate capacitance of 37.2fF, which is similar to the analytical calculation of the upstate capacitance is 32.5fF. Similarly, the downstate capacitance is extracted from the isolation losses, the theoretical and calculated values of isolation are similar at ($f < f_0/5$) that is 4GHZ. Consider the resonant frequency value below 4GHZ that is 3 GHz, and the isolation value is 16dB. This isolation value gives the downstate capacitance of 2.8pF, similar to the calculated down state capacitance of 2.6PF. Bridge resistance and inductance values are extracted from the isolation losses at resonant frequency 20GHz, and the MEMS bridge produces isolation of -64dB. This value of isolation can extract the bridge resistance 2.4 Ω . Similarly, the inductance value is extracted at a frequency of 50GHz, and this value is -30dB. This isolation value can extract the bridge inductance 21.9 pH; the analytical and extracted values of resistance, inductance and capacitance are shown in Table3.

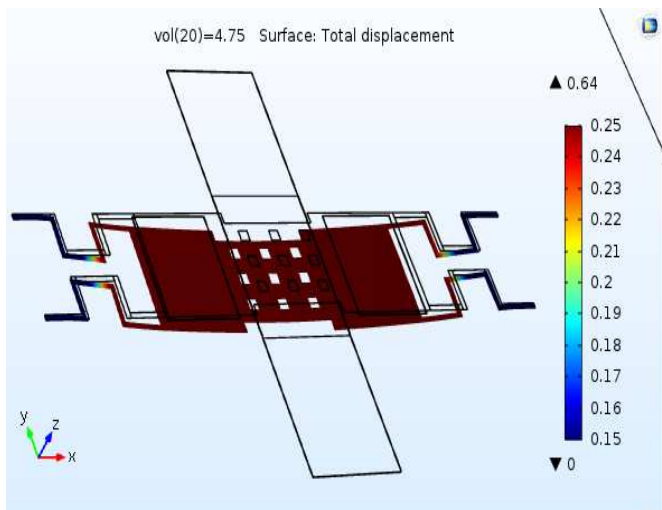
3. Results and Discussions

3.1 Pull-In Voltage of Final Proposed Structure

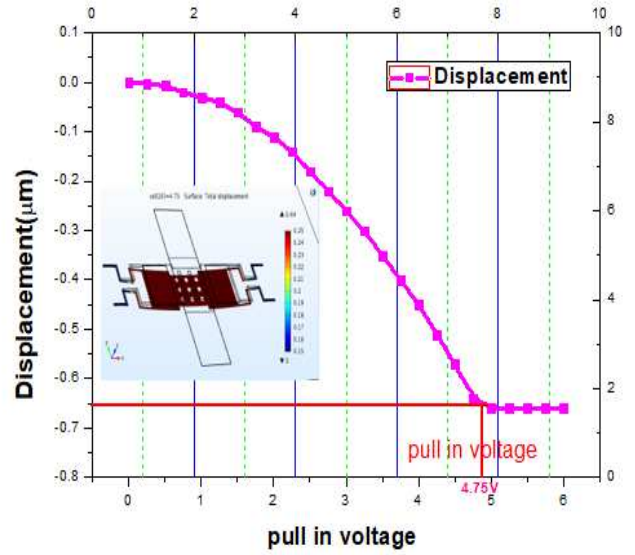
The COMSOL FEM tool simulated the proposed final RF MEMS switch. The actuation voltage is applied between the lower electrode and beam; voltage difference between the beam and electrodes increases the electrostatic force that pull the beam down. Capacitance is formed between the beam and signal line because of the dielectric layer. Electrostatic actuation mechanism used to change the state of the switch from ON state to OFF state. DC voltage is used to actuate the RF MEMS shunt switch. The minimum voltage required to collapse the beam on the signal line is known as pull-in voltage. The Pull-in voltage of the final proposed RF MEMS shunt switch is calculated analytically by Eq. (13). According to the applied actuation voltage, the displacement of the beam is represented in Fig15.

$$V_p = \sqrt{\frac{8kg_0^3}{27\epsilon_0 A}} \quad (13)$$

Where k is the spring constant of the structure, g_0 =air gap between the beam and the signal line, ϵ_0 =relative permittivity of free space is $\epsilon_0 = 8.85 * 10^{-12} F / m$, and A is actuation area. The actuation area of the proposed switch is calculated as $A = (2(W * w) + (w_s * w_b))$. Where W, w, w_s , and w_b are widths of the beam, electrode, signal line, and width of the beam, respectively. $A = (2(W * w) + (w_s * w_b))$.



(a)

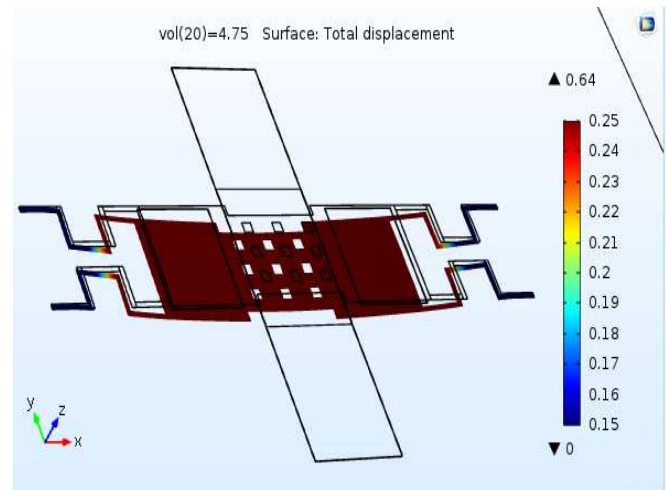


(b)

Fig.15 a Simulated of RF MEMS switch, b pull-in voltage of proposed switch

3.2 Effect of Beam Material on The Pull-In Voltage

Different materials are available to select the beam material, and the most used materials are gold, aluminium, copper, platinum, nickel. The beam material influences the pull-in voltage, RF losses of the proposed switch. Material indices are defined by their properties, such as young's modulus (E), electric resistivity (ρ), thermal expansion coefficient (α), Poisson's ratio (ν), and thermal conductivity (k). Different material indices are observed with other materials and it is found that Au, Al, Si are the best materials for beam. Gold has a limitation regarding its high cost and aluminium is also good for selecting beam material, but it has a drawback, that is it's highly reactive with moisture and forms rust, which impacts the switch's lifetime. Gold is the best material for selecting the beam. The pull-in voltage of different beam materials of the RF MEMS switch is Al, Au, Cu, Ti, and Ni is 4.45V, 4.75V, 5.5V, 5.58V and 7.5V in Fig.16a. The pull-in voltage of the Al is very low compared to the gold, however, due to the limitation of Al, gold is prepared for beam material.



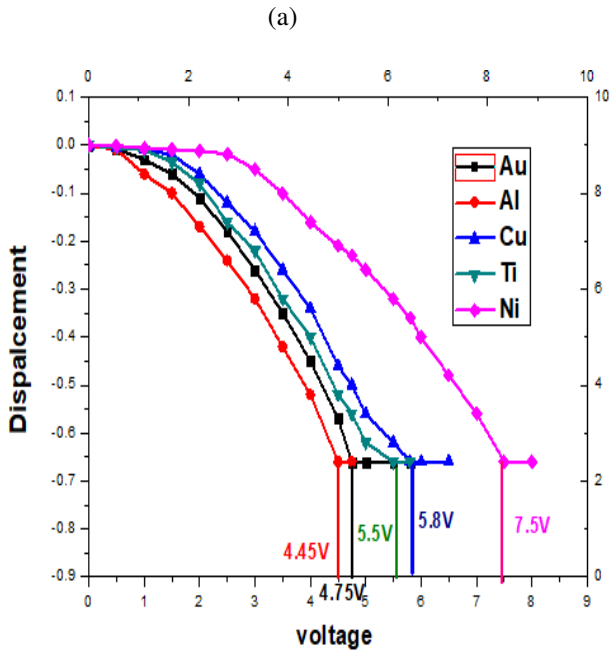


Fig.16a Simulation of proposed switch, **b** Analysis of pull-in voltage for different beam materials

3.3. Effect of Beam Thickness and Air Gap on Pull-in Voltage

The thickness of the beam plays an important role in decreasing the pull-in voltage by reducing the spring constant K . The spring constant of the beam is proportional to the beam thickness shown in Eq.(14).

$$k \propto t^3 \quad (14)$$

K = spring constant, t = thickness of the beam, the thickness of the beam is varying from $0.5\mu\text{m}$ to $2\mu\text{m}$. The RF performances of the switch were observed at a different thickness of the beam, good return losses are observed at $1\mu\text{m}$ and $2\mu\text{m}$ compared to $0.5\mu\text{m}$ and $1\mu\text{m}$. The calculated spring constant of the beam at $1\mu\text{m}$ and $2\mu\text{m}$ is more than 3 times, when compared the spring constant of the beam at thickness $0.5\mu\text{m}$, and $1.5\mu\text{m}$, hence the thickness of $0.5\mu\text{m}$ is selected. The spring constant of the beam decreases while selecting the small beam thickness and long length; lower the switch spring constant affects the pull-in voltage. The effect of beam thickness on the pull-in voltage of the proposed switch is shown in Fig.17a. pull-in voltage of the RF MEMS shunt switch is proportional to the air gap between the beam and the signal line. The air gap in general rise from $1.5\mu\text{m}$ to $4\mu\text{m}$, if air gap is increased then pull in voltage of the switch increases, and less air gap condition produces the sticking problem while in actuation. The effect of the air gap on the MEMS switch's pull-in voltage for different air gaps is shown in Fig.17b.

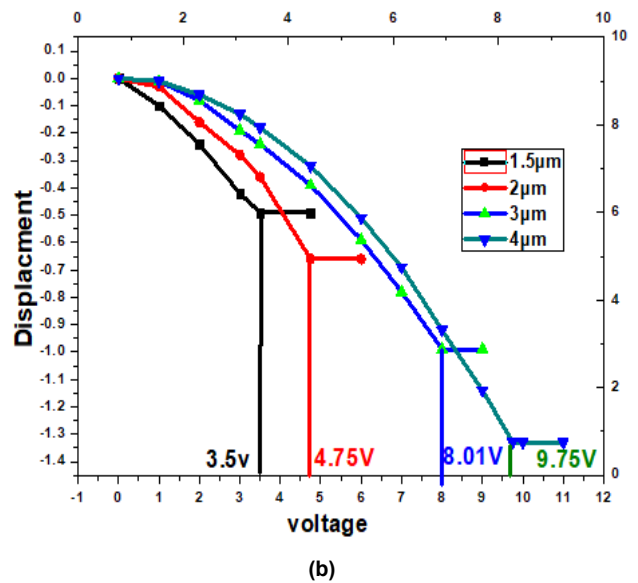
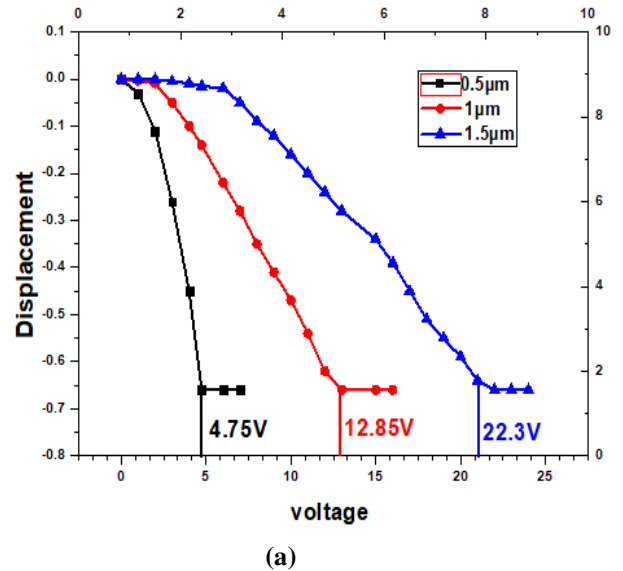


Fig.17a Pull-in voltage analysis of RF MEMS switch for different thickness of the beam, **b** Analysis of pull-in voltage for different air gap

3.4 Effect of Dielectric Materials and Dielectric Thickness on The Pull in Voltage.

The dielectric material selection for RF MEMS switch depends on the different material properties such as dielectric constant, electric resistivity, thermal conductivity, thermal expansion coefficient, and young's modulus. The reliability of the RF MEMS switch depends on the charging and discharging of the dielectric material (Sravani K. G et al. 2019). The most frequently used dielectric materials are HfO_2 , Si_3N_4 and SiO_2 , among all, Si_3N_4 is preferred for dielectric material for MEMS switch because of easy deposition at low temperature. There is not that great effect on the pull-in voltage while changing the different dielectric material. The effect of changing dielectric material on the pull-in voltage is shown in Fig.18a, the dielectric material thickness also has less impact on the pull-in voltage. The pull-in voltage of the RF MEMS switch for different

thicknesses of dielectric is shown in Fig.18b. The thickness of the dielectric varies in the range of $0.1\mu\text{m}$ to $2\mu\text{m}$, excellent RF losses are observed at $0.3\mu\text{m}$ (Sravani K. G et al.2019).

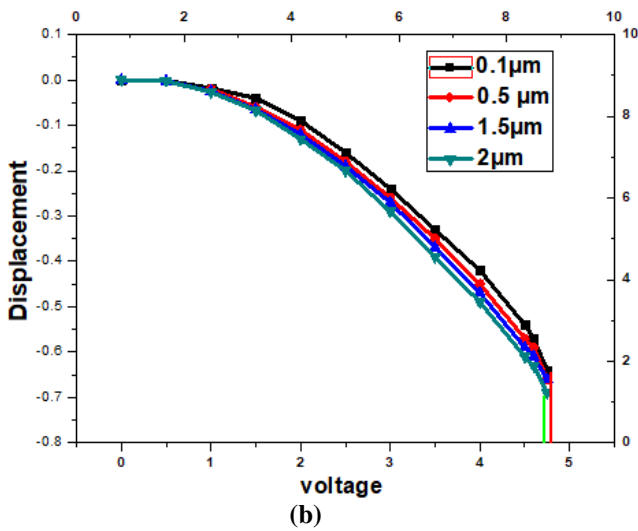
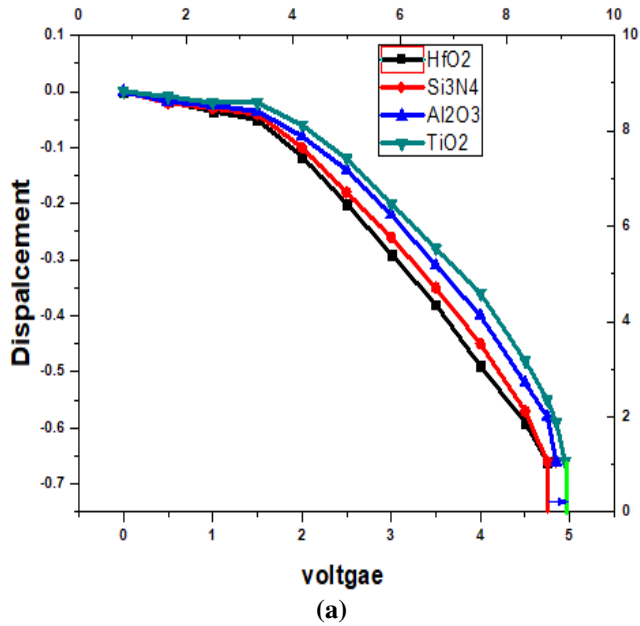


Fig.18aEffect of pull-in voltage of RF MEMS switch for different dielectric materials, **b**Effect of pull-in voltage of RF MEMS switch for different thickness of the dielectric materials

3.5 Stress Analysis

The spring constant, stress of the RF MEMS switch is analysed by using the FEM tool. The analytical model needs different Equations for different types of structures; hence, the FEM tool must find the spring constant and pull-in voltage (Singh, T. et al. 2015). Gold membranes withstand the maximum stress of 100Mpa. The maximum stress of the gold membrane exhibits by applying a force of $1.02\mu\text{N}$ as shown in Fig.19. Beyond the maximum force is applied breakdown condition has occurred in the gold membrane.

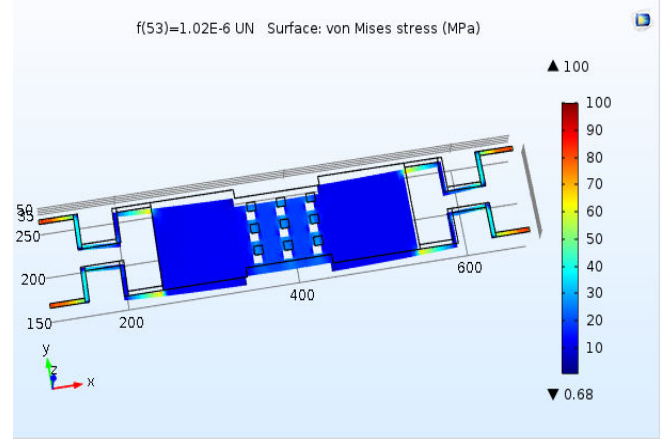


Fig.19 The maximum stress 100Mpa is showing at the maximum force of $1.02\mu\text{N}$

The maximum force required to displace the $0.6\mu\text{m}$ is $0.2\mu\text{N}$, which is less than the maximum total force of $10.2\mu\text{N}$ as shown in Fig.20. maximum and minimum stress values of the gold membrane is varied from the 0.13-19.4Mpa at $0.6\mu\text{m}$ displacement force, which is less than the total stress withstand by the gold membrane. Therefore, the gold membrane will not be exhibiting the breakdown condition at $0.2\mu\text{N}$ as shown in Fig.21.

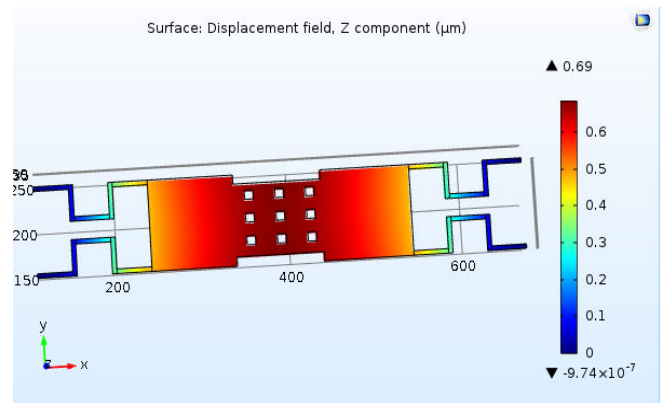


Fig.20The maximum displacement of $0.6\mu\text{m}$ at maximum force of $0.2\mu\text{N}$

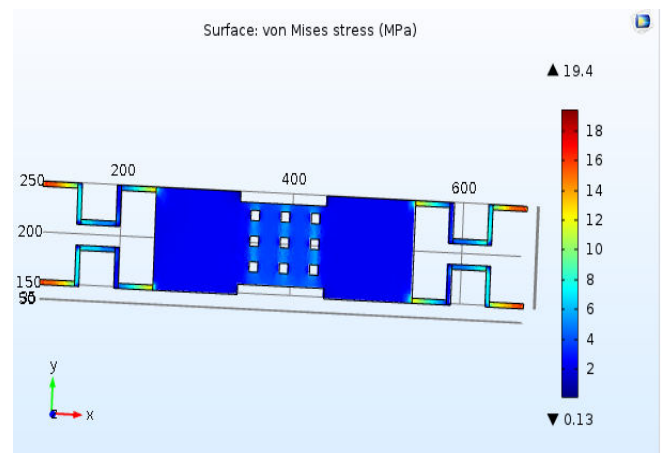


Fig.21Stress distribution of capacitive switch of 0.6 displacements at maximum force of $0.2\mu\text{N}$

3.6 Spring Constant

The maximum holding force of the membrane is applied to the beam, and the corresponding deflections are noted. The ratio of displacement of the membrane according to the applied voltage gives the membrane spring constant. The simulated spring constant value of the proposed RF MEMS switch is 0.68N/m^2 as shown in Fig.22, which is similar to the analytical spring constant value. Spring constant of membrane plays a key role in determining pull-in voltage.

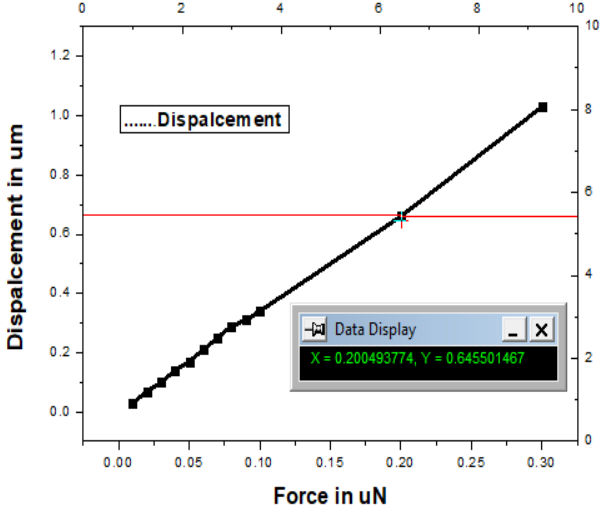


Fig.22 Force vs displacement Conway the spring constant of the proposed shunt switch

3.7 Capacitance Analysis

The RF performance of the proposed MEMS shunt switch depends on the capacitance ratio. The capacitance ratio of the RF MEMS switch is the ratio of downstate capacitance to upstate capacitance. The RF MEMS switch membrane is placed over a CPW signal line, which regulates the flow of the RF signal in the CPW signal line. While no biasing is applied, a small capacitance is present between the membrane and the signal line. This capacitance is called upstate capacitance. This capacitance does not have the capability to ground the signal. C_{on} or C_{up} is the upstate capacitance measured when the switch is in ON position by Eq.(15).

$$C_{on} = \frac{\epsilon_0 A}{g_0 + \frac{t_d}{\epsilon_r}} \quad (15)$$

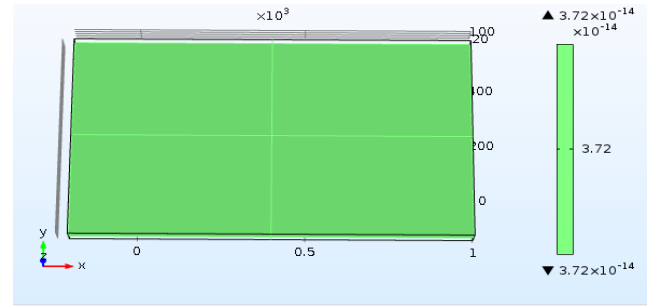
ϵ_0 is the permittivity of free space, ϵ_r is the relative permittivity of dielectric material, g_0 is an air gap, t_d is the thickness of the dielectric layer, and A is the overlapping area. RF MEMS shunt switch shows different capacitance for different materials because the relative permittivity is not the same for all materials (Sravani K. G; Narayana et al. 2018). The up-state capacitance varies according to the air gap, and upstate capacitance decreases while increasing the

air gap, and vice-versa. Biasing is applied between the electrodes; the membrane vertically deflects and touches the signal line reducing the air gap between the beam and the signal line. The capacitance value increases, and RF MEMS offers a high impedance to transmit the RF signal to the output port. C_{off} or C_{down} is the downstate capacitance, measured when the switch is in OFF state position by Eq. (16).

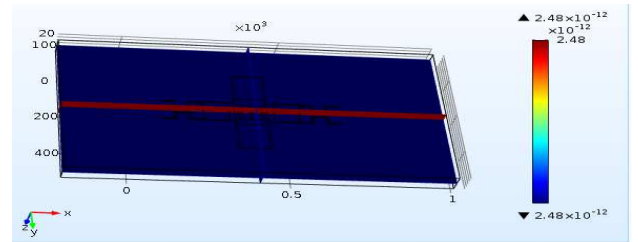
$$C_{off} = \frac{\epsilon_0 \epsilon_r A}{t_d} \quad (16)$$

A is the overlapping area between the membrane and signal line of CPW and the overlapping area between the beam and electrodes. The proposed switch is simulated with the help of electrostatic physics module in the COMSOL FEM tool. Voltage is applied to the electrodes and signal line in both ON and OFF state positions. Simulated results of proposed upstate and downstate capacitance are shown in Fig.23. Simulated and analytical values of ON-state and OFF-state capacitance are 32.2 fF, 31.2fF, and 2.62pF, 2.42pF, respectively. Analytical and simulated values of upstate and downstate capacitance are similar. The capacitance ratio of the proposed RF MEMS shunt switch is calculated by Eq.(17).

$$C_{ratio} = \frac{\frac{\epsilon_0 \epsilon_r A}{t_d}}{g_0 + \frac{t_d}{\epsilon_r}} \quad (17)$$



(a)



(b)

Fig.23 Simulated capacitance of proposed device **a** Upstate capacitance, **b** Downstate capacitance

The capacitance value of all the proposed switches is represented in Table 4. The final proposed switch meanders with perforation exhibit a more capacitance ratio compared to the other proposed switches.

Table 4 The comparison of capacitance for proposed switches

Sl.no	Proposed switch	Cup(pF)	C _{down} (fF)	Capacitance ratio
1	Plane beam	44.05	6.64	151.25
2	H shaped	35.2	5.31	150.4
3	Perforations along with meanders	31.25	2.66	170.25

The thickness of the dielectric on both on-state and off-state capacitance of the proposed device is shown in Fig.23.

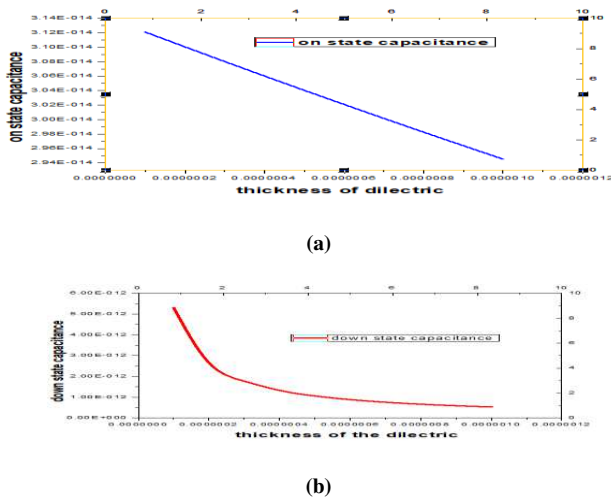


Fig.24. Effect of thickness of the beam **a**On state capacitance, **b**Off-state capacitance

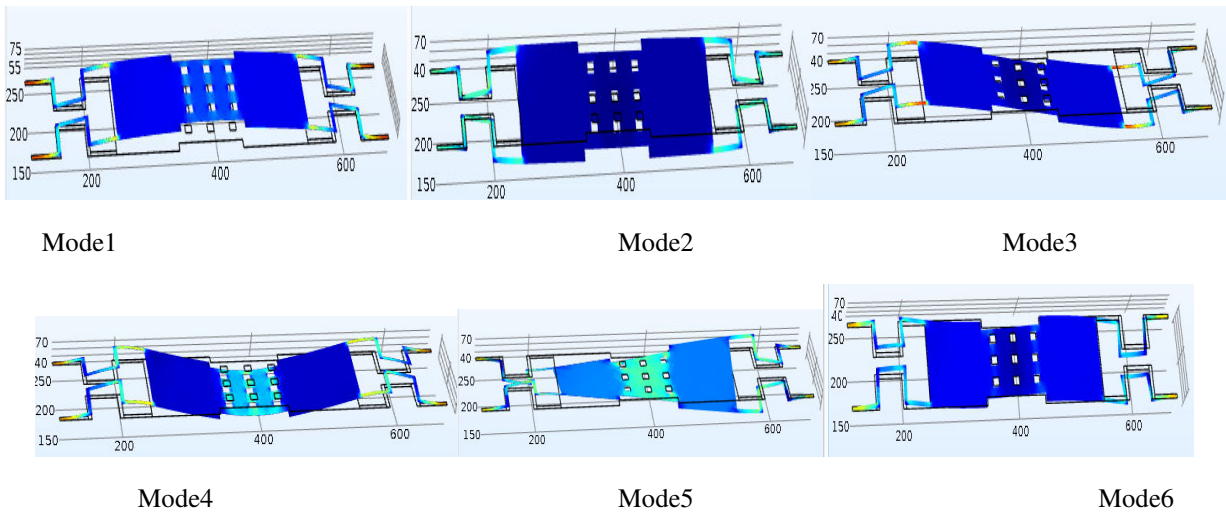


Fig.25 Vibrating modes of shunt membrane of RF MEMS switch

3.8 Frequency Model Analysis

The eigenfrequency analysis of the proposed switch is done by the FEM tool, to obtain the resonant frequency of the switch, harmonic modes of the membrane under the applied force can be derived by carrying out eigenfrequency analysis. Model frequency of the proposed switch is obtained by solving the Lagrange of the system and then applying the canonical equation (Chu C. H et al. 2007). The harmonic motion of the membrane can be derived by Modelling the second-order mass spring damper system by Eq.(18).

$$F_E = M_{efe} \frac{d^2x}{dt^2} + \gamma_{efe} \frac{dx}{dt} + Kx \quad (18)$$

M_{efe} = effective mass of membrane, γ_{efe} = effective damping coefficient of dielectric material, F_E = electro static force generated, Kx = overall spring constant. From all the six vibrating modes, model 1 is suitable for the proposed device. The resonant frequency of proposed model1 is 27.2KHZ, rest of all the modes produce the uneven rise and fall. The signal transmission efficiency is more in model1 compared to the other modes because uneven capacitance noise is more in all modes except in mode1. The stress of model1 is 36.89 MPA, which is within the limits of stress developed before buckling. All the six modes of vibrations are shown in Fig.25.

3.9 Resonant Frequency Analysis

Resonant frequency is affected by the Spring constant and proof mass of the beam; mechanical vibration of the beam (Rao K. S. et al. 2018) can be calculated by Eq. (19).

$$f_0 = \frac{1}{2\pi} \sqrt{\frac{k}{m}} \quad (19)$$

m is the mass of the beam ($m=0.35*(L*w*t*d)$), d is the density of beam $3.355*10^{-13}$ kg/m³. proof mass and spring constant is fixed, vibrating in the structure, varying the spring constant that affects resonant frequency. The analytical calculation of the resonant frequency of the proposed RF MEMS shunts switch is 28.5 KHz.

3.10 Quality Factor

The reliability of the RF MEMS switch is examined by using the quality factor. The value of the quality factor is changed from 0.5 to 2. A switch with quality factor below 0.5, has a low switching characteristic, and greater than 2 shows low settling time. Transmission line resistance and beam resistance decrease the quality factor and substrate resistance increase the quality factor. T-line, beam, and substrate resistivity effect on quality factors at peak values. Downstate capacitance affects the quality factor at peak values. The analytical value of quality factor for fixed-fixed RF MEMS switch at room temperature is 1.2.

$$Q.F = \frac{k}{\omega_0 b} = \frac{\sqrt{\epsilon \rho t^2 g_0^3}}{\mu \left(\frac{wl}{2}\right)^2} \quad (20)$$

μ = coefficient of viscosity, k is the total spring constant, ω_0 is the mechanical resonant frequency, b is the damping ratio.

3.11 Switching Time Analysis

Switching time is one of the important parameters of the RF MEMS shunt switch. The switching time of the proposed switch affects the working of transmission and receiving applications. Time taken by the beam to deflect from upstate to downstate is known as switching time. The switching time of the proposed switch is calculated by Eq.(21).

$$T_s = \frac{3.67V_p}{\omega_0 V_s} \quad (21)$$

T_s = switching time, V_p = pull in voltage, V_s = actuation voltage, ω_0 = resonant frequency of membrane.

The ratio of the pull-in voltage to actuation voltage is constant, that is 1.4, switching time mainly depends on the resonant frequency. The switching time of the proposed RF MEMS shunt switch is 16 μ s.

3.12 Electromagnetic Analysis

DC voltage is applied between the two electrodes, electrostatic force is generated, and the beam is pulled down and collapsed on the signal line. Parallel plate capacitance is induced in between the beam and signal line. The scattering parameters of the proposed device, such as return losses (S_{11}), insertion losses (S_{12}), and isolation losses (S_{21}) are measured by the HFSS 13.0V and ADS tool. Insertion losses and return losses are measured ON-state condition, and isolation losses were measured in OFF-state position. The proposed device is ON state, and exhibits low insertion losses and return losses when the signal is transmitting. In ON state insertion losses (S_{11}) depends on the impedance matching of the device. The amount of RF power radiated back to the input terminals is called return losses, generally return losses are <-10dB. The proposed RF MEMS shunt switch return losses are -38.4dB at 0.5GHZ and -10dB at 35.2GHZ during the switch is on the state (Sravani K. G et al. 2018). The return loss of the switch depends on the air gap; the effect of the air gap on the return losses is shown in Fig.26.

$$S_{11} = \frac{-j\omega_0 C_u Z_0}{2 + j\omega C_u Z_0}, \quad (S_{11} < -10\text{dB}) \quad (22)$$

$$|S_{11}|^2 = \frac{\omega^2 C_u^2 Z_0^2}{4} \quad (23)$$

ω_0 = resonant frequency, C_u = upstate capacitance, Z_0 = input impedance is 50 Ω .

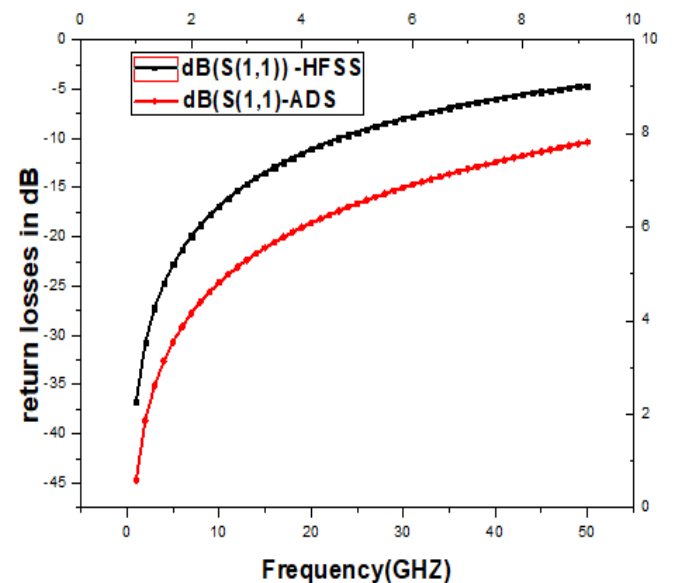


Fig.26 The return losses of the proposed switch at 0.5 to 50GHz range during on state

Insertion losses of RF MEMS shunt switch take place refraction of signal from the signal line, and the measured value of the device is generally below 1dB. Insertion losses of the proposed device are shown in Fig.27 insertion losses of the switch is due to the substrate properties. High dielectric constant materials reduce the insertion losses (Srivani K. G;Prathyusha et al.2020).

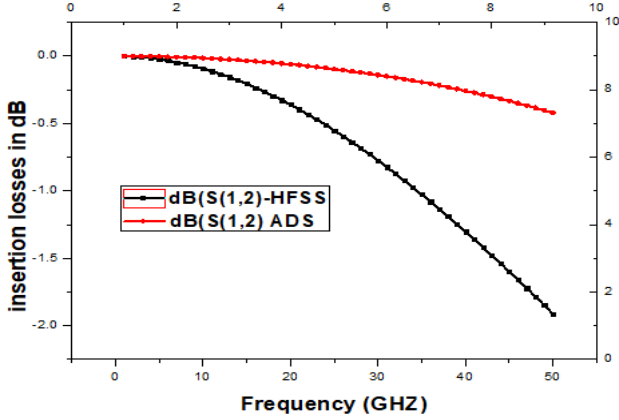


Fig 27 Insertion losses of proposed switch 0.5 to 50 GHz range during on state

Isolation losses occur when the switch is in OFF position, that beam is collapsed on the signal line. The switch's downstate capacitance plays a key role in attenuating the RF signal from the input port to the output port. The proposed RF MEMS switch exhibits an isolation of -65dB at 20GHz central frequency. Switch exhibits good isolation in the frequency range of 18-26 GHz.

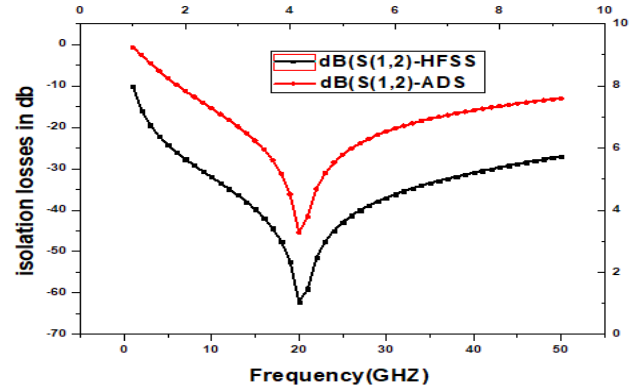


Fig.28 Isolation losses of the proposed switch

Table 5 Comparison of RF losses in ADS AND HFSS

Rf Loses	ADS	HFSS
Insertion losses(S_{12})	0.1dB	0.1dB
Return losses (S_{11})	48dB	37.5dB
Isolation losses(S_{21})	45dB	65dB

The RF performance of the proposed switch is studied in both ADS and HFSS tools. Good insertion and return losses are observed in the ADS and excellent isolation losses are exhibited in the HFSS. The simulated values of RF losses are as shown in Table 5.

3.13. Comparison of proposed RF MEMS switch with literature survey

The proposed switch shows excellent mechanical and RF performance while comparing with the existing results shown in Table 6.

Table 6 The comparison of the proposed switch with previous literature

component	Ref.(Sudhanshu Shekhar et al. 2017)	Ref. (Hamid Reza Ansari et al.2018)	Ref.(Yasser Mafinejad et al. 2018))	Ref. (G.Shanthi et al. 2020)	Proposed work (2021)
Substrate	Silicon	Silicon	Silicon	Silicon	Silicon
Dielectric layer		SiO ₂	SiO ₂	SiO ₂	Si ₃ N ₄
Membrane	Au	Al	Gold	Gold	Gold
Electrode thickness(μ m)		2	1-1.2	2	1.5
Pull in voltage(V)	4.8-6.3	2.2	18-25	5.2	4.75
Switching time (μ s)	< 20	3	23.1	16
C _d	1.6-2	17.2	2.6
C _{up}	0.1-0.13	42.5	31.2
C _d /C _{up} ratio	12-20	170
Return losses(dB)	11.47	>10	0.1	36.3
Insertion losses (dB)	0.25	0.85	0.9	<0.1	0.15
Isolation losses (dB)	30-40	71	14	42.11	68

4. Conclusions

In this paper, evaluating the MEMS shunt switch and the final proposed device with perforations and uniform meanders. Different shapes of beams and meandering techniques are evaluated to reduce the pull-in voltage and spring constant of the proposed switch. The effect of perforation on the RF MEMS shunt was also evaluated in the paper. The final proposed switch has a low actuation voltage and good RF performance such as low insertion loss, return loss, and high isolation loss. In this paper, all the analysis of the final proposed switch RF MEMS shunt switch are done using electromechanical study, quality factor, capacitance, mechanical stress, switching time, eigenfrequency analysis, and scattering parameters.

For the proposed device the pull-in voltage is obtained as 4.75V with uniform meanders, and the switching time is 16 μ s. From the capacitance analysis, the upstate, downstate capacitance, and capacitance ratios are 31.2fF, 2.6pF and 170, respectively. Beam material used for the switch is gold for high dielectric conductivity, low weight for high switching speed. Silicon nitride (Si_3N_4) is used as a dielectric layer for high isolation. The proposed switch exhibits good RF performances in the K band application; hence the proposed device can be used in K band satellite applications for fast switching applications.

Acknowledgment

The authors would like to thank NMDC, supported by NPMAS, National Institute of Technology, Silchar, for providing the necessary computational tools.

REFERENCES

- Rebeiz, G. M. (2004). RF MEMS: theory, design, and technology. John Wiley & Sons.
- Sharma, P., Perruisseau-Carrier, J., Moldovan, C., & Ionescu, A. M. (2013) Electromagnetic performance of RF MEMS graphene capacitive switches. *IEEE transactions on nanotechnology* 13(1) : 70-79.
- Rebeiz, G. M., & Muldavin, J. B (2001) RF MEMS switches and switch circuits. *IEEE Microwave magazine* 2(4) :59-71.
- Daneshmand, M., Fouladi, S., Mansour, R. R., Lisi, M., & Stajcer, T (2009) Thermally actuated latching RF MEMS switch and its characteristics. *IEEE Transactions on Microwave Theory and Techniques* 57(12): 3229-3238.
- Sharma, Kuldeep, et al (2020). Design and characterization of RF MEMS capacitive shunt switch for X, Ku, K and Ka band applications. *Microelectronic Engineering* (2020): 111310.
- Sravani, K. G., Guha, K., & Rao, K. S (2020). Analysis of a novel RF MEMS switch using different meander techniques. *Microsystem Technologies* 26(5) :1625-1635.
- Koutsourelis, M., Adikimenakis, A., Michalas, L., Papandreou, E., Stavrinidis, G., Konstantinidis, G., ... & Papaioannou, G (2014) Comparative study of AlN dielectric films electrical properties for MEMS capacitive switches. *Microelectronic engineering* 130: 69-73.
- Chakraborty, Amrita, and Bhaskar Gupta (2017) Utility of RF MEMS miniature switched capacitors in phase shifting applications. *AEU- International Journal of Electronics and Communications* 75 : 98-107.
- Peroulis, Dimitrios, Sergio P. Pacheco, and Linda PB Katehi (2004) RF MEMS switches with enhanced power-handling capabilities. *IEEE Transactions on Microwave Theory and Techniques* 52(1): 59-68.
- Sravani, K. G., Narayana, T. L., Guha, K., & Rao, K. S (2018) Role of dielectric layer and beam membrane in improving the performance of capacitive RF MEMS switches for Ka-band applications. *Microsystem Technologies* 1-10.
- Majumder, S., Lampen, J., Morrison, R., & Maciel, J. (2003) A packaged, high-lifetime ohmic MEMS RF switch. *IEEE MTT-S International Microwave Symposium Digest* (Vol. 3, pp. 1935-1938).
- Topalli, K., Unlu, M., Atasoy, H. I., Demir, S., Aydin Civi, O., & Akin, T. (2009) Empirical Eq.tion of bridge inductance in inductively tuned RF MEMS shunt switches. *Progress In Electromagnetics Research* 97: 343-356.
- Narayana, T. L., Sravani, K. G., & Rao, K. S. (2017) Design and analysis of CPW based shunt capacitive RF MEMS switch. *Cogent Engineering* 4(1): 1363356.
- Sravani, K. G., Prathyusha, D., Gopichand, C., Maturi, S. M., Elsinawi, A., Guha, K., & Rao, K. S. (2020) Design, simulation and analysis of RF MEMS capacitive shunt switches with high isolation and low pull-in-voltage. *Microsystem Technologies*: 1-16.
- Ansari, Hamid Reza, and Mojtaba Behnam Taghaddosi (2019) Optimization and development of the RF MEMS structures for low voltage, high isolation and low stress. *Analog Integrated Circuits and Signal Processing* 101.(3) : 659-668.
- Kumar, P. A., Rao, K. S., Balaji, B., Aditya, M., Maity, N. P., Maity, R., ... & Sravani, K. G. (2021) Low Pull-in-Voltage RF-MEMS Shunt Switch for 5G Millimeter Wave Applications. *Transactions on Electrical and Electronic Materials*: 1-12.
- Ansari, Hamid Reza, and Saeed Khosroabadi. (2019) Design and simulation of a novel RF MEMS shunt capacitive switch with a unique spring for Ka-band application. *Microsystem Technologies* 25(2): 531-540.
- Sharma, A. K., & Gupta, N. (2013) Microelectromechanical system (MEMS) switches for radio frequency applications-a review. *Sensors & Transducers* 148(1):1- 11.
- Singh, T. (2015) Design and finite element modeling of series-shunt configuration based RF MEMS switch for high isolation operation in K-Ka band. *Journal of Computational Electronics* 14(1):167-179.
- Marcelli, R., Lucibello, A., De Angelis, G., Proietti, E., & Comastri, D. (2010) Mechanical modelling of capacitive RF MEMS shunt switches. *Microsystem technologies* 16(7): 1057-1064.
- Kumar, P. A., Rao, K. S., Sravani, K. G., Balaji, B., Aditya, M., Guha, K., & Elsinawi, A. (2021). An Intensive Approach to Optimize Capacitive type RF MEMS Shunt Switch. *Microelectronics Journal* 112: 105050.
- Sravani, K. G., Guha, K., & Rao, K. S. (2020) Analysis of a novel RF MEMS switch using different meander techniques. *Microsystem Technologies* 26(5): 1625-1635.
- Chakraborty, A., Gupta, B., & Sarkar, B. K. (2014) Design, fabrication and characterization of miniature RF MEMS switched capacitor based phase shifter. *Microelectronics Journal*, 45(8): 1093-1102.10
- Sravani, K. G., Guha, K., & Rao, K. S. (2018) Analysis on selection of beam material for novel step structured RF-MEMS switch used for satellite communication applications. *Transactions on Electrical and Electronic Materials* 19(6): 467-474.
- Chu, C. H., Shih, W. P., Chung, S. Y., Tsai, H. C., Shing, T. K., & Chang, P. Z. (2007) A low actuation voltage electrostatic actuator for RF MEMS switch applications. *Journal of micromechanics and microengineering* 17(8): 1649
- Saxena, A., & Agrawal, V. K. (2015) Comparative study of perforated RF MEMS switch. *Procedia Computer Science* 57: 139-145.
- Shanthi, G., Srinivasa Rao, K., & Girija Sravani, K. (2020) Design and analysis of a RF MEMS shunt switch using U-shaped meanders for low actuation voltage. *Microsystem Technologies*: 1-9.
- Mafinejad, Y., Kouzani, A., Mafinezhad, K., & Hosseinezhad, R. (2017) Low insertion loss and high isolation capacitive RF MEMS switch with low pull-in voltage. *The International Journal of Advanced Manufacturing Technology* 93(1): 661-670.
- Ansari, H. R., & Khosroabadi, S. (2019) Design and simulation of a novel RF MEMS shunt capacitive switch with a unique spring for Ka-band application. *Microsystem Technologies* 25(2): 531-540.
- Shekhar, S., Vinoy, K. J., & Ananthasuresh, G. K. (2017) Surface-micromachined capacitive RF switches with low actuation voltage and steady contact. *Journal of Microelectromechanical Systems* 26(3): 643-652.
- Sravani, K. G., Guha, K., & Elsinawi, A. (2019) Design and optimisation of a novel structure capacitive RF MEMS switch to integrate with an antenna to improve its performance parameters. *IET Circuits, Devices & Systems* 14(3):276-287.

- Sharma, A. K., & Gupta, N. (2015) Electromagnetic modeling and parameter extraction of RF-MEMS switch. *Microsystem Technologies*21(1) 181-185.
- Sravani, K. G., Prathyusha, D., Rao, K. S., Kumar, P. A., Lakshmi, G. S., Chand, C. G., ... & Guha, K. (2019) Design and performance analysis of low pull-in voltage of dimple type capacitive RF MEMS shunt switch for Ka-band. *IEEE Access*7: 44471-44488.